université PARIS DIDEROT PARIS 7

TIME EVOLUTION OF PROTOPLANETARY DISKS : SNOW REGIONS AND TIME DEPENDENT PLANET TRAPS.

CD-1

K. Baillié (kevin.baillie@cea.fr) and S. Charnoz

Laboratoire AIM, Université Paris Diderot / CEA / CNRS, 91191 Gif-sur-Yvette, France.

HD97048, Lagage et al., 2007

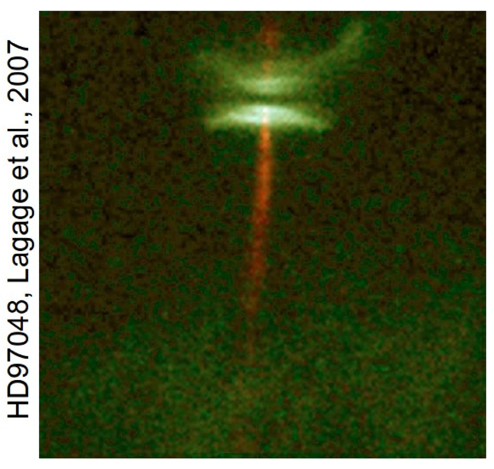

Abstract

In order to model the favorable conditions for planetary formation, we have designed a hydrodynamical numerical model for the spreading of protoplanetary disks based on a self-consistent coupling between the disk thermodynamics, photosphere geometry and dynamics (Baillié & Charnoz., 2014, ApJ 786, 35). We retrieved the recurrent observational properties of protoplanetary disks around young Classical T Tauri type stars. The proper treatment of the disk geometry lead to the apparition of non-irradiated zones. Here, we show the importance of the disk composition: using a full-opacity model, our disk temperature takes into account the various changes of phases of the disk components. This is crucial for estimating the resonant torques that a planet would experience: corotation and Lindblad torques are very sensitive to the discontinuities in surface-mass density and temperature gradients. From these torques, we show that there are some preferential zones for planetary embryos to accumulate and that some regions could be totally depleted in planetary cores.

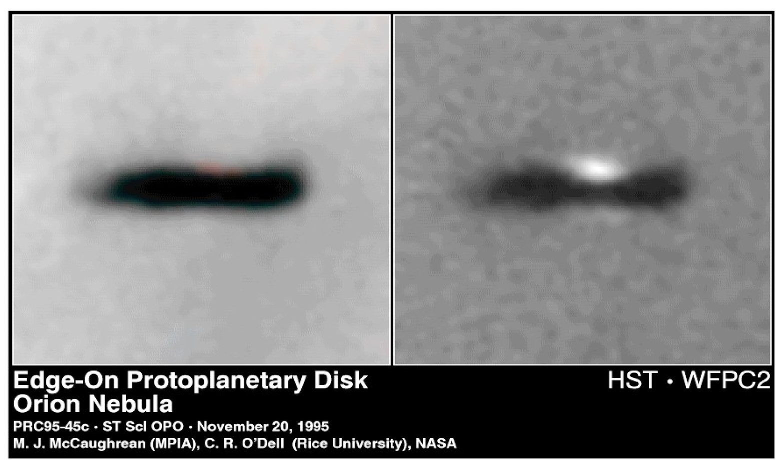

Problematic

- Disk lifetime ~ a few 10^6 years (Beckwith & Sargent, 1996, Hartmann et al., 1998)
- Type I inward migration ~ 10^5 years (Artymowicz, 1993, Ward, 1997)
- Planetary formation ~ 10^{6-7} years (Pollack et al., 1996)

Need to slow down inward migration.

Possible planet trapping at 0-torque radii (Lyra et al., 2010, Bitsch & Kley, 2011, Hasegawa & Pudritz, 2011)

Can the proper treatment of temperature and geometry provide favorable conditions for planet trapping ?

Model

1D + 1D numerical viscous spreading hydrodynamical code from Baillié & Charnoz, 2014.

Evolution of an initial Minimum Mass Solar Nebula :

- **irradiation heating + viscous heating + radiative cooling**
- **coupling dynamics & thermodynamics (turbulent viscosity)**
- **coupling temperature & photosphere geometry (→ shadowing)**
- **realistic opacity model (Semenov et al., 2003)**

$$\alpha_{grazing} \rightarrow T \rightarrow h_{pressure} \rightarrow H_{photosphere} \rightarrow \frac{dH_{ph}}{dr} \rightarrow \alpha_{grazing}$$

$T \rightarrow \nu \rightarrow$ viscous spreading

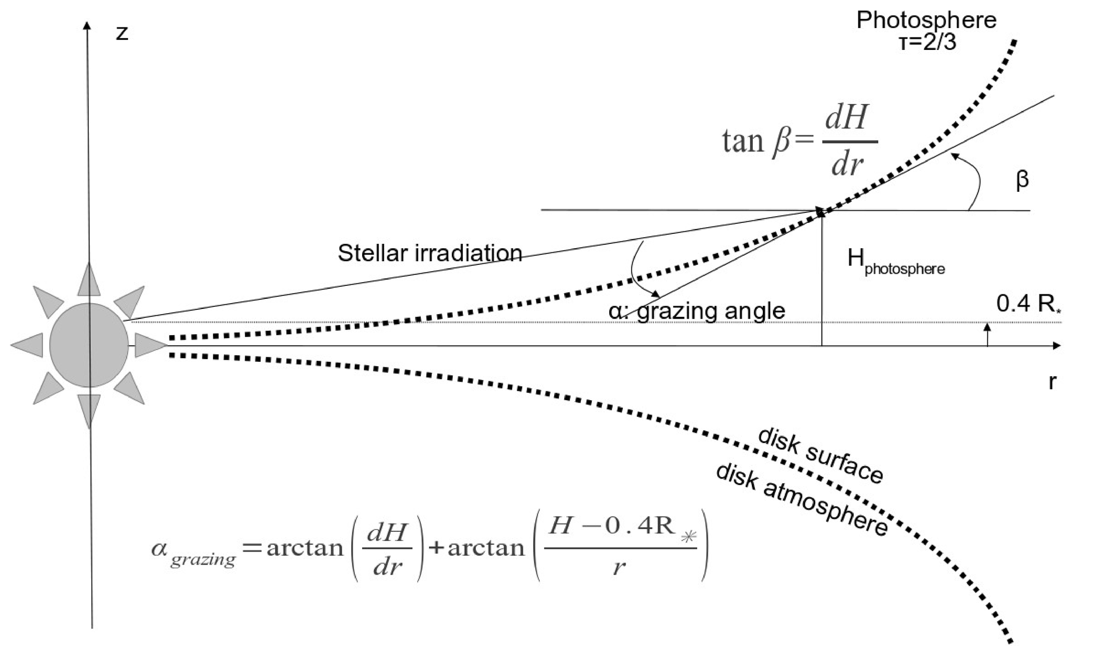

$$\alpha_{grazing} = \arctan\left(\frac{dH}{dr}\right) + \arctan\left(\frac{H - 0.4R_{\odot}}{r}\right)$$

Figure 1 : Geometric model of an irradiated protoplanetary disk.

$$\frac{\partial \Sigma}{\partial t} = \frac{3}{r}\frac{\partial}{\partial r}\left(\sqrt{r}\frac{\partial}{\partial r}\left(\nu \Sigma \sqrt{r}\right)\right)$$ Lynden-Bell and Pringle, 1974

Influence of the disk composition on the midplane temperature

Opacity reflects the **phases** of the disk components as a function of the temperature. Strong influence of the water ice and silicate sublimation.

- Steady state, uniform mass flux : $\Sigma \propto r^{-1}$ // Observations (Andrews et al., 2009, Isella et al., 2009)
- **Temperature plateaux** at $T_{sublimation}$
- **Gradient discontinuities** in surface mass density and temperature.

Elements	Condensation / Sublimation Temperature
Water ice	160 K
Volatile organics	275 K
Refractory organics	425 K
Troilite FeS	680 K
Olivine, pyroxene ([Fe,Mg] silicates)	1500 K

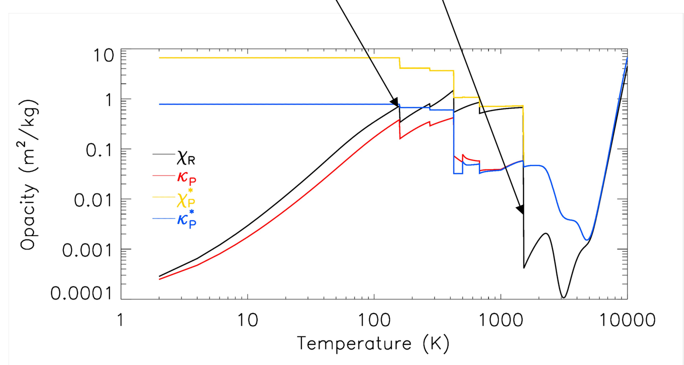

Figure 2 : Opacity variations with local temperature (from Semenov et al., 2003)

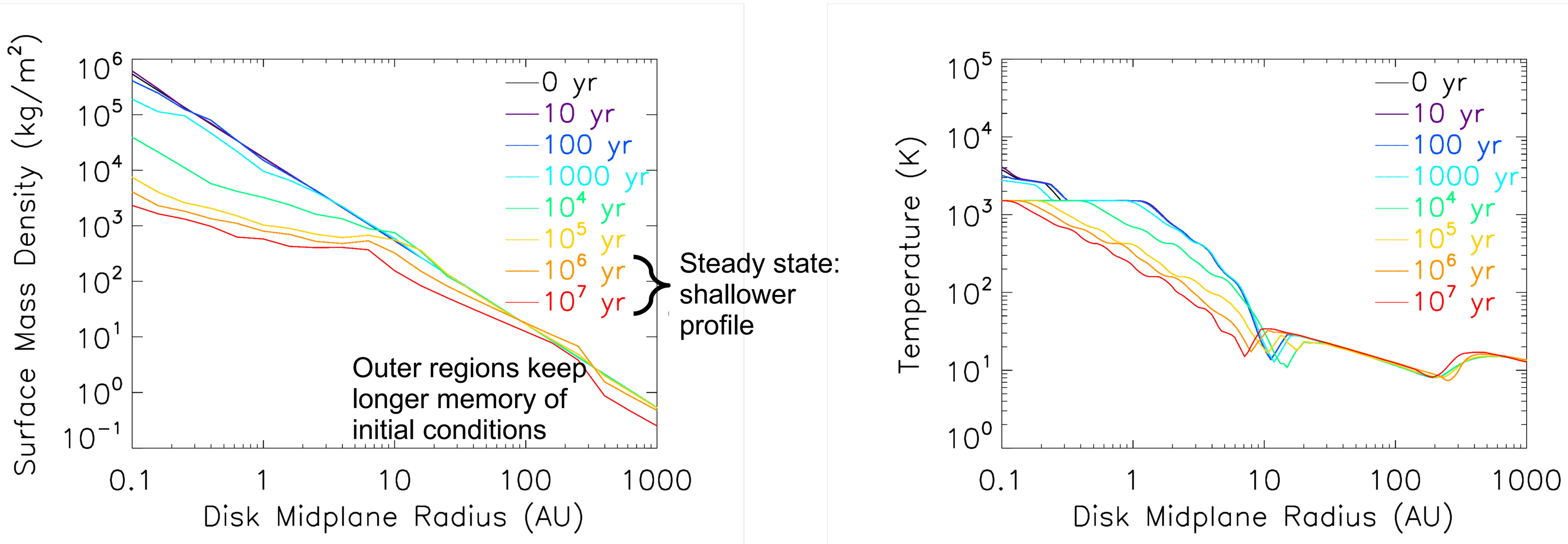

Figure 3 : Evolution of the surface-mass density and temperature radial profiles for an initial MMSN.

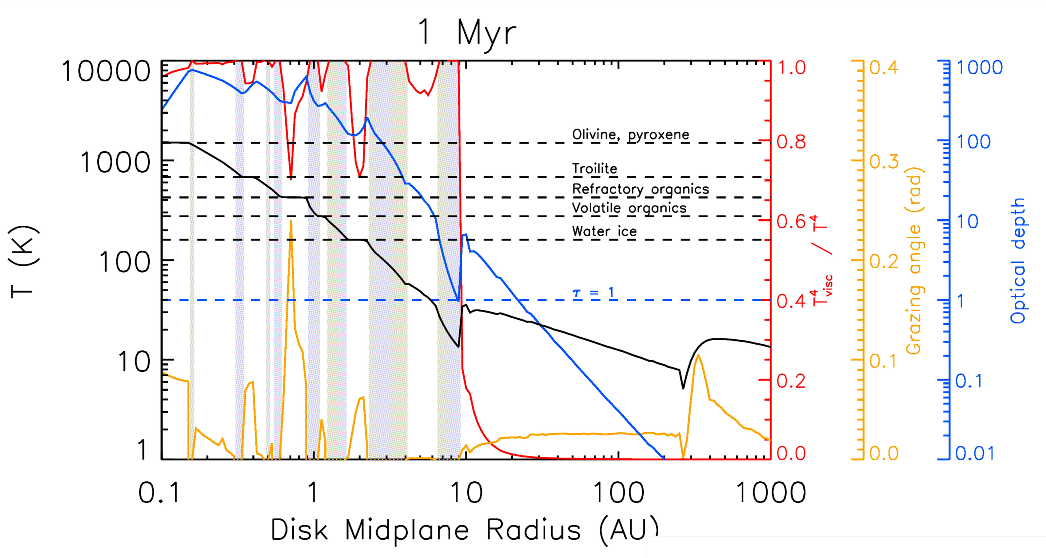

Figure 4 : Mid-plane temperature radial profile after 1 Myr. Shadowed regions in gray. The ratio of the viscous heating contribution over the total heating is presented in red, the grazing angle profile in yellow and the optical depth profile in blue.

- **Shadowed regions** outside the temperature plateaux
- Sharp edge at the heat transition barrier
- **Enlarged snow and sublimation zones, migrating inward.**

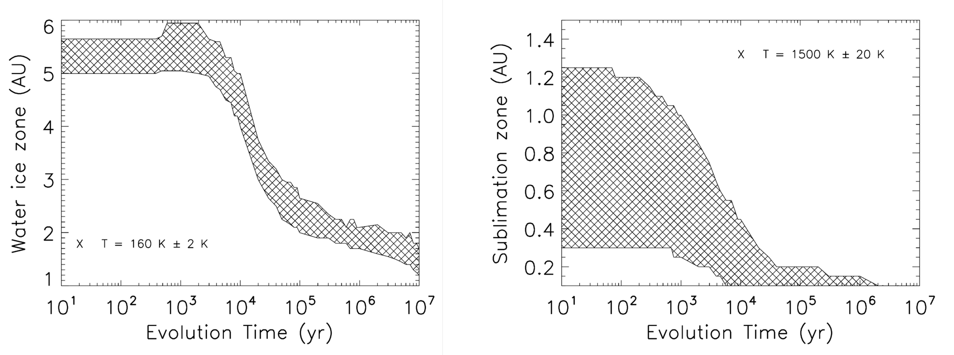

Figure 5 : Time evolution of the snowzone and sublimation zone positions.

Planetary migration torques

Lindblad torque :

A planetary embryo interacts with the disk, create spiral density waves at resonance locations and yield angular momentum to the disk → inward type I migration.

Goldreich & Tremaine, 1979, Ward, 1997, Hasegawa & Pudritz, 2011b

Wavenumber ~ continuous function of r → torque density

$$\Gamma_{\mathrm{Lindblad}} = -\int_r \int_{-H_{photo}}^{+H_{photo}} \frac{\partial^2 \Gamma}{\partial z \partial r} \mathrm{d}r\mathrm{d}z \approx -4\, h_{pres} \int_r \frac{\partial^2 \Gamma}{\partial z \partial r} \mathrm{d}r\mathrm{d}z$$

Corotation torque (horseshoe drag) may slow down or reverse migration.

Ward, 1991, Paardekooper et al., 2010, Bitsch et al., 2014

$$\Gamma_{\mathrm{hs,entro}} = -\frac{\Gamma_0(r_P)}{\gamma^2} 7.9 \left(-\frac{\partial \ln T}{\partial \ln r}(r_P) + (\gamma - 1)\frac{\partial \ln \Sigma}{\partial \ln r}(r_P)\right)$$

$$\Gamma_{\mathrm{hs,baro}} = -\frac{\Gamma_0(r_P)}{\gamma} 1.1 \left(\frac{\partial \ln \Sigma}{\partial \ln r}(r_P) + \frac{3}{2}\right)$$

$$\Gamma_{\mathrm{total}} = \Gamma_{\mathrm{Lindblad}} + \Gamma_{\mathrm{hs,baro}} + \Gamma_{\mathrm{hs,entro}}$$

Very sensitive to Σ and T gradients.

Directly estimated from the hydrodynamical evolution rather than from power-law fits.

For a 10 $M_{\oplus}$ planet in an initial MMSN.

$\Gamma_{Lindblad} > 0$ for 8.8 < r < 9.8 AU & 10.8 < r < 11.4 AU

$\Gamma_{corotation}$ alternatively > 0 and < 0

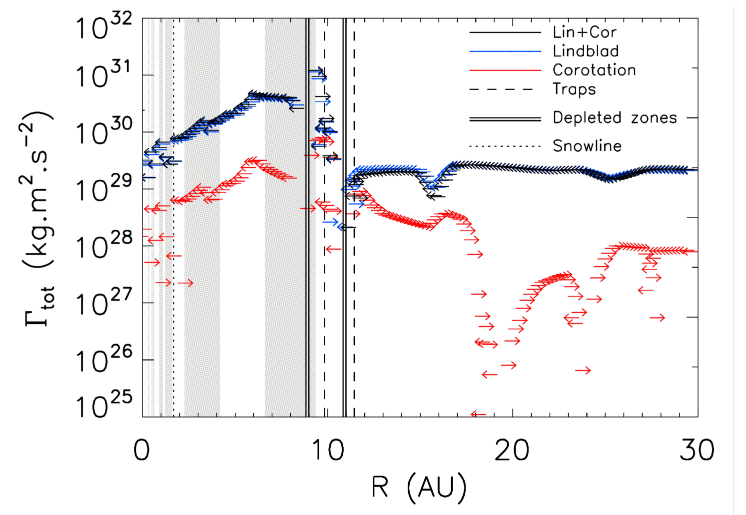

Figure 6 : Radial profile of the Lindblad, corotation and total torques after 1 Myr for M_P=10 $M_{\oplus}$. Gray: shadowed regions.

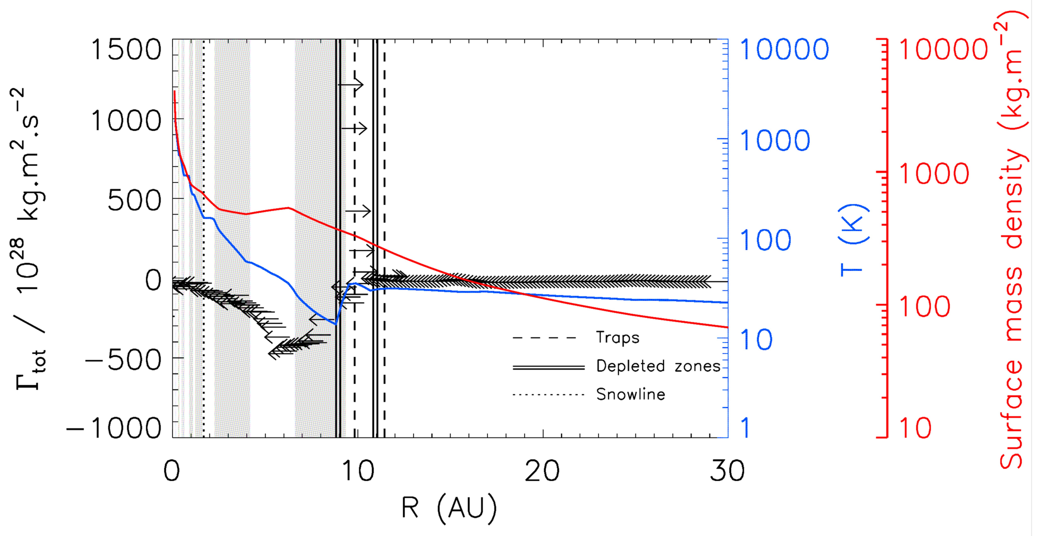

Figure 7 : Radial profile of the total torque after 1 Myr with temperature and surface mass density radial profiles. Shadowed regions are displayed in gray.

0-torque radius ~ equilibrium radius

- traps at 9.8 AU & 11.4 AU
- deserts at 8.8 AU & 10.8 AU

// Bitsch et al., 2011 : eq. radius at 12.5 AU for 20 $M_{\oplus}$-planet.

Eq. radius correlated with density and temperature irregularities.

- **Multiple migrating trap and desert populations**
- **Traps at r ~ 1 AU until 1000 yr**
- **Correlation between a desert population and the heat transition barrier**

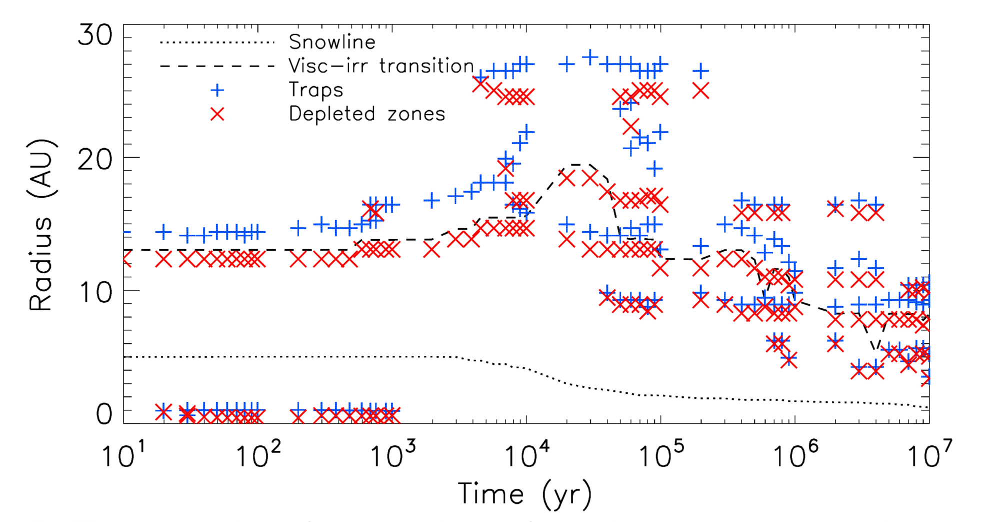

Figure 8 : Time evolution of the locations of the planetary traps and deserts.

Conclusions

- **Steady state reached in ~ 1 Myr : observationnal constraints retrieved**
- **Temperature plateaux at the disk components phase changes**
- **Enlarged snowline migrating inward and stabilizing below 2 AU**
- **Migration torques are very sensitive to Σ and T gradients**
- **Realistic geometry and disk composition favor planet traps and deserts**

Perspectives

- Molecular cloud collapse + proto-sun evolution
- Photo-evaporation
- Variable turbulent viscosity, deadzones
- Observationnal characterization of temperature plateaux and shadowed regions
- Multiple planets

References

S. M. Andrews, D. J. Wilner, A. M. Hughes, C. Qi, and C. P. Dullemond. Protoplanetary Disk Structures in Ophiuchus. ApJ, 700:1502–1523, Aug. 2009.
P. Artymowicz. On the Wave Excitation and a Generalized Torque Formula for Lindblad Resonances Excited by External Potential. ApJ, 419:155, Dec. 1993.
K. Baillié and S. Charnoz. Time Evolution of a Viscous Protoplanetary Disk with a Free Geometry: Toward a More Self-consistent Picture. ApJ, 786:35, May 2014.
S. V. W. Beckwith and A. I. Sargent. Circumstellar disks and the search for neighbouring planetary systems. Nature, 383:139–144, Sept. 1996.
B. Bitsch and W. Kley. Range of outward migration and influence of the disc's mass on the bmigration of giant planet cores. A&A, 536:A77, Dec. 2011.
B. Bitsch, A. Morbidelli, E. Lega, and A. Crida. Stellar irradiated discs and implications on migration of embedded planets. II. Accreting-discs. A&A, 564:A135, Apr. 2014.
P. Goldreich and S. Tremaine. The excitation of density waves at the Lindblad and corotation resonances by an external potential. ApJ, 233:857–871, Nov. 1979.
L. Hartmann, N. Calvet, E. Gullbring, and P. D'Alessio. Accretion and the Evolution of T Tauri Disks. ApJ, 495:385, Mar. 1998.
Y. Hasegawa and R. E. Pudritz. The origin of planetary system architectures - I. Multiple planet traps in gaseous discs. MNRAS, 417:1236–1259, Oct. 2011.
A. Isella, J. M. Carpenter, and A. I. Sargent. Structure and Evolution of Pre-main-sequence Circumstellar Disks. ApJ, 701:260–282, Aug. 2009.
D. Lynden-Bell and J. E. Pringle. The evolution of viscous discs and the origin of the nebular variables. MNRAS, 168:603–637, Sept. 1974.– 47 –
W. Lyra, S.-J. Paardekooper, and M.-M. Mac Low. Orbital Migration of Low-mass Planets in Evolutionary Radiative Models: Avoiding Catastrophic Infall. ApJ, 715:L68–L73, June 2010.
S.-J. Paardekooper, C. Baruteau, A. Crida, and W. Kley. A torque formula for non- isothermal type I planetary migration - I. Unsaturated horseshoe drag. MNRAS, 401:1950–1964, Jan. 2010.– 48
J. B. Pollack, O. Hubickyj, P. Bodenheimer, J. J. Lissauer, M. Podolak, and Y. Greenzweig. Formation of the Giant Planets by Concurrent Accretion of Solids and Gas. Icarus, 124:62–85, Nov. 1996.
D. Semenov, T. Henning, C. Helling, M. Ilgner, and E. Sedlmayr. Rosseland and Planck mean opacities for protoplanetary discs. A&A, 410:611–621, Nov. 2003.
W. R. Ward. Horsehoe Orbit Drag. In Lunar and Planetary Science Conference, volume 22 of Lunar and Planetary Science Conference, page 1463, Mar. 1991.
W. R. Ward. Protoplanet Migration by Nebula Tides. Icarus, 126:261–281, Apr. 1997.